

GPD PROGRAM AT COMPASS

N. D'HOSE* for the COMPASS Collaboration

*CEA, Centre de Saclay
Irfu/SPhN, 91191 Gif-sur-Yvette, France
E-mail: nicole.dhose@cea.fr

The study of exclusive reactions like Deeply Virtual Compton Scattering (DVCS) and Meson Production is one major part of the future COMPASS program¹ in order to investigate nucleon structure through Generalised Parton Distributions (GPD). The high energy of the muon beam allows to measure the x_B -dependence of the t -slope of the pure DVCS cross section and to study nucleon tomography. The use of positive and negative polarised muon beams allows to determine the Beam Charge and Spin Difference of the DVCS cross sections to access the real part of the Compton form factor related to the dominant GPD H.

Keywords: Nucleon Structure, Generalised Parton Distributions, Deeply Virtual Compton Scattering

1. Kinematic domain provided by COMPASS

The COMPASS apparatus is located at the unique CERN SPS M2 beam line that is able to deliver high-energy (50-280 GeV) and highly-polarised μ^\pm particles. It consists of a high-resolution forward spectrometer and an unpolarised, longitudinally or transversely polarised target. By installing a recoil proton detector around a liquid hydrogen target to ensure exclusivity of the Deeply Virtual Compton Scattering (DVCS) and Deeply Virtual Meson Production (DVMP) events, COMPASS would become a facility measuring exclusive reactions within a kinematic domain ranging from $x_B \sim 0.01$ to about 0.1, which cannot be explored by any other existing or planned facility in the near future (Fig. 1). COMPASS would thus explore the uncharted x_B domain between the HERA collider experiments H1 and ZEUS and the fixed-target experiments as HERMES and the planned 12 GeV extension of the JLab.

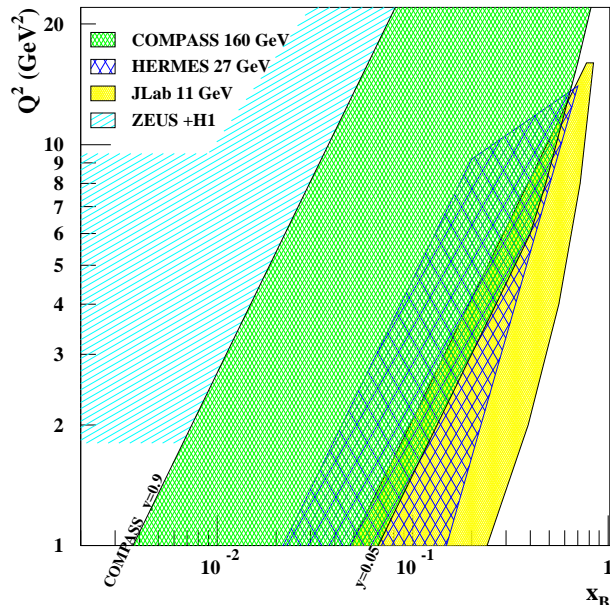


Figure 1. Kinematic domains for measurements of hard exclusive processes shown for the COMPASS (green area enclosed by the lines $y = 0.9$ and $y = 0.05$), HERMES and JLab fixed-target experiments and the HERA collider experiments H1 and ZEUS. COMPASS will explore the uncharted territory in between the collider region and that of the lower-energy fixed-target HERMES and JLab experiments.

2. Methodology for DVCS with high energy polarised μ^+ and μ^- beams

Deeply Virtual Compton Scattering has the same final state as the competing Bethe–Heitler (BH) process, which is elastic lepton–nucleon scattering with a hard photon emitted by either the incoming or outgoing lepton. The differential cross section for hard exclusive muoproduction of real photons off an unpolarised proton target can be written as^a

$$\frac{d^4\sigma(\mu p \rightarrow \mu p \gamma)}{dx_B dQ^2 d|t| d\phi} = d\sigma^{BH} + (d\sigma_{unpol}^{DVCS} + P_\mu d\sigma_{pol}^{DVCS}) + e_\mu (\text{Re } I + P_\mu \text{Im } I), \quad (1)$$

^aFor simplicity $d\sigma$ is used in the following instead of $\frac{d^4\sigma(\mu p \rightarrow \mu p \gamma)}{dx_B dQ^2 d|t| d\phi}$.

where P_μ is the polarisation and e_μ the charge in units of the elementary charge, of the polarised muon beam. The interference term I arises as the DVCS and BH processes interfere on the level of amplitudes.

COMPASS offers the advantage to provide various kinematic domains where either BH or DVCS dominate (see Fig. 2). The Bethe-Heitler am-

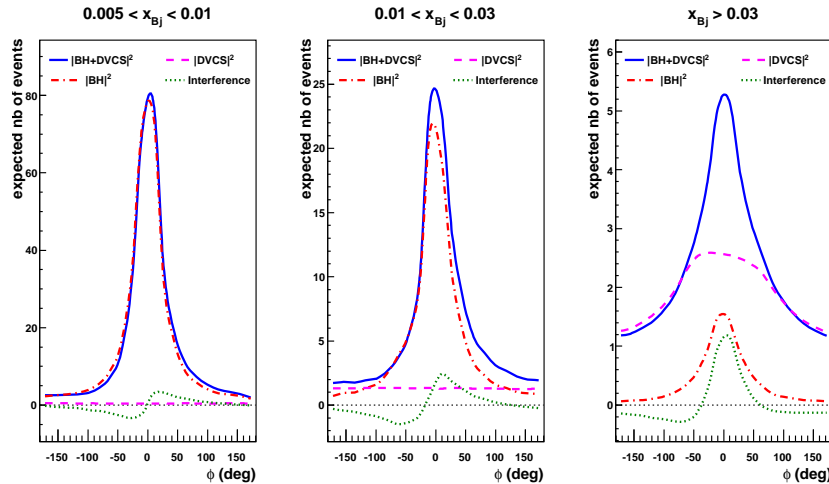


Figure 2. Monte Carlo simulation of the exclusive process $\mu^+ p \rightarrow \mu'^+ p \gamma$ for $Q^2 > 1 \text{ GeV}^2$, showing the ϕ angle distribution for three bins in x_B : $0.005 < x_B < 0.01$ (left), $0.01 < x_B < 0.03$ (middle) and $0.03 < x_B$ (right). The event yield shown is normalised to the integrated luminosity of the 2009 DVCS test run, as described in Sect. 5. It is based on the acceptance of the presently existing COMPASS set-up, *i.e.*, using the existing calorimeters ECAL1 and ECAL2.

plitude is well known (it relies only on the knowledge of elastic nucleon form factors). The collection of almost pure BH events at small x_B allows one to get an excellent reference yield and to control accurately the global efficiency of the apparatus. In contrast the collection of almost pure DVCS events at larger x_B will allow the measurement of the x_B -dependence of the t -slope of the cross section which is related to the tomographic partonic image of the nucleon. In the intermediate domain, the DVCS contribution will be boosted by the BH process through the interference term. COMPASS is presently the only facility to provide polarised leptons with either charge: polarised μ^+ and μ^- beams. As the BH is independent of

charge and polarisation, this contribution can be removed by subtracting 2 separate measurements obtained for the two beam charges. Moreover the natural polarisation of the muon beam produced from pion decay changes sign when the beam charge is reversed and the different topologies of μ^+ and μ^- , polarised with opposite direction, allows one to select only the real part or the imaginary part of the complex amplitude of DVCS.

3. Beam Charge and Spin Difference of the DVCS cross sections to determine the real part of the Compton form factor \mathcal{H}

The Beam Charge (C) and Spin (S) Difference for Unpolarized (U) proton can be written as:

$$\begin{aligned} \mathcal{D}_{CS,U} \equiv d\sigma^{\rightarrow} - d\sigma^{\leftarrow} &= 2[P_{\mu}d\sigma_{pol}^{DVCS} + e_{\mu}\text{Re } I] \\ &\propto \left(\{s_1^{DVCS} \sin \phi\} \right) + \left(c_0^I + c_1^I \cos \phi + \{c_2^I \cos 2\phi + c_3^I \cos 3\phi\} \right) \end{aligned} \quad (2)$$

in which the BH contribution *cancels out*. In this formula, the DVCS amplitude is expanded in $1/Q$ beyond leading twist-2 including all twist-3 contributions.² The coefficients c_n^{DVCS} and s_n^I are related to certain combinations of Compton Form Factors (CFFs). A CFF \mathcal{F} is a sum over flavors f , of convolutions of the respective GPDs F^f with a perturbatively calculable kernel describing the hard γ^*q interaction. Note that each contribution in Eq. 2 and Eq. 3 shown between a pair of braces corresponds to higher-twist or higher-order effects. The analysis of the ϕ -dependence of the beam charge and spin difference $\mathcal{D}_{CS,U}$ will provide via the term $\text{Re } I$ the two leading twist-2 expansion coefficients c_0^I and c_1^I . In COMPASS kinematics they are mainly related to the *real* part of the Compton form factor \mathcal{H} that is in LO given by a flavor sum of convolutions involving the GPDs H^f *i.e.* $\text{Re}\mathcal{H}^f = \mathcal{P} \int_{-1}^{+1} \frac{H^f(x,\xi,t)}{x-\xi} dx$. In fact the GPDs depend upon three kinematic variables: t the total four-momentum squared transferred between initial and final nucleon states, x and $\xi \sim x_B/(2-x_B)$ respectively average and half the difference between the initial and final longitudinal momentum fractions of the nucleon, carried by the partons throughout the process. In hard exclusive processes as DVCS, x is then an internal variable which is integrated over in a convolution.

Fig. 3 shows the projected statistical accuracy in a particular (x, Q^2) bin, for a measurement of the ϕ -dependence of the beam charge and spin difference $\mathcal{D}_{CS,U}$. Two of the curves are calculated using the ‘‘VGG’’ GPD model.³ The model based on a ‘‘reggeized’’ parameterisation of the corre-

lated x, t dependence of the GPDs uses a shrinkage parameter α' to describe the decrease in nucleon size with increasing x . As this model is meant to be applied mostly in the valence region, typically a large value $\alpha' = 0.8$ is used. For comparison, also the model for the “factorized” x, t dependence is shown, which corresponds to $\alpha' \approx 0.1$ in the ‘reggeized’ ansatz. A recent theoretical development exploits dispersion relations for Compton form factors. In this context, the additional curve is the result of a fitting procedure⁴ including next-to-next-to leading order (NNLO) corrections which was developed and successfully applied to describe DVCS observables from very small values of x_B , for the HERA collider to large x_B for HERMES and JLab. It has to be noted that the real part of the Compton form factor \mathcal{H} was found positive at H1 and ZEUS and negative at HERMES and JLab. The COMPASS kinematic domain is expected to provide the node of the real part of this amplitude, which is an essential input for any global fit analysis.

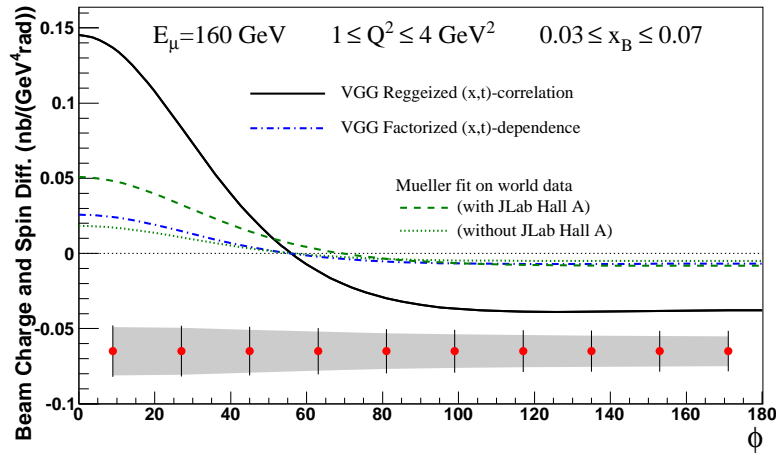


Figure 3. Projected statistical (error bars) and systematic (grey band) accuracy for a measurement of the ϕ dependence of the Beam Charge and Spin Difference at COMPASS for $0.03 \leq x \leq 0.07$ and $1 \leq Q^2 \leq 4 \text{ GeV}^2$ and for 280 days of running time with a 2.5m LH₂ target, an intensity of $4.6 \times 10^8 \mu$ in a 48 s SPS spill period and an overall *global efficiency* $\epsilon_{global} = 0.1$. The solid and dash-dotted curves correspond to different variants of the VGG model³ while the dashed and dotted curves show predictions based on first fits on world data.⁴

4. x_B -dependence of the t -slope of the pure DVCS cross section to study nucleon tomography

The Beam Charge and Spin Sum of cross sections can also be evaluated:

$$\begin{aligned} \mathcal{S}_{CS,U} \equiv d\sigma^{\leftarrow} + d\sigma^{\rightarrow} &= 2[d\sigma^{BH} + d\sigma_{unpol}^{DVCS} + e_{\mu}P_{\mu}\text{Im } I] \\ &\propto 2[d\sigma^{BH}] + \left(c_0^{DVCS} + \{c_1^{DVCS} \cos \phi + c_2^{DVCS} \cos 2\phi\} \right) \\ &\quad + \left(s_1^I \sin \phi + \{s_2^I \sin 2\phi\} \right) \end{aligned} \quad (3)$$

in which the BH contribution *does not cancel out*.

- (1) The analysis of the ϕ -dependence of the beam charge and spin sum $\mathcal{S}_{CS,U}$ will provide via the term $\text{Im } I$ the leading twist-2 quantity s_1^I . Its dominant contribution is related to the *imaginary* part of the Compton form factor \mathcal{H} , *i.e.* $\text{Im}\mathcal{H}^f \propto H(\xi, \xi, t)$.
- (2) A parallel analysis can be performed subtracting the BH contribution when it is not too large, and integrating over ϕ to get rid of the complete interference term and of the ϕ -dependent terms of the DVCS contribution. Thus the DVCS leading twist-2 quantity c_0^{DVCS} can be isolated and its characteristic t -slope can be determined as a function of x_B , from which conclusions can be drawn on the evolution of transverse size of the nucleon over the x_B -range accessible to COMPASS. Such a mapping in x_B is referred to as “Nucleon Tomography”.

Fig. 4 shows the projected statistical accuracy for a measurement at COMPASS of the x_B -dependence of the t -slope parameter $B(x_B)$ of the DVCS cross section. In the simple ansatz $\frac{d\sigma}{dt} \propto \exp(-B(x_B)|t|)$ and $B(x_B) = B_0 + 2\alpha' \log(\frac{x_B}{x})$. At small x_B , where amplitudes are predominantly imaginary, the overall transverse size of the nucleon $\langle r_{\perp}^2(x_B) \rangle \approx 2 \cdot B(x_B)$. Data on B exist only for the HERA collider x_B -range from 10^{-4} to 0.01,^{5,6} below the COMPASS range $0.01 < x_B < 0.1$. No evolution with x_B was observed and a first transverse proton radius has been determined $\langle r_{\perp}^2 \rangle = 0.65 \pm 0.02$ fm using H1 data.⁵ In the valence region, where no experimental determinations of B exist, some information comes from fits adjusted to form factor data which give $\alpha' \simeq 1$ GeV².^{7,8} For the simulation two values $\alpha' = 0.125$ and $\alpha' = 0.26$ are shown which correspond to the half and the total of the value for Pomeron exchange in soft scattering processes. The largest value can be determined with an accuracy better than 2.5 sigma by using the two existing calorimeters ECAL1 and ECAL2 while the smallest value requires a new ECAL0 to get a better precision at large x_B .

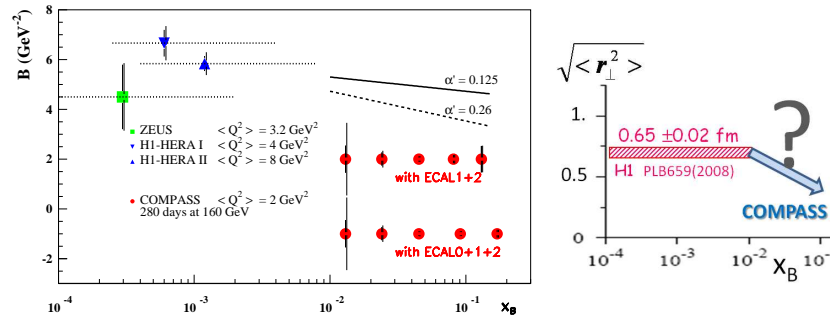


Figure 4. Left: Projections for measuring the x_B dependence of the t -slope parameter $B(x_B)$ of the DVCS cross section, calculated for $1 < Q^2 < 8 \text{ GeV}^2$. For comparison some HERA results with similar $\langle Q^2 \rangle$ are shown.^{5,6} The left vertical bar on each data point indicates the statistical error only while the right one includes also the systematic uncertainty, using only ECAL1 and ECAL2 (first row) and also ECAL0 (second row). Two different parameterisations are shown using $\alpha' = 0.125 \text{ GeV}^{-2}$ and 0.26 GeV^{-2} . **Right:** Transverse proton radius as a function of x_B . New and significant information will be obtained in the uncharted x_B region, further elucidating the issue of “nucleon tomography”.

5. First Observation of BH and DVCS events in 2008 and 2009 tests

A preliminary study of the feasibility of DVCS measurements was performed in 2008 and 2009 with minimum disturbance of the ongoing hadron spectroscopy measurements. The experimental set-up makes use of the 40 cm long LH₂ target, surrounded by a Recoil Proton Detector (RPD). It includes all detectors presently available including the ECAL1 and ECAL2 electromagnetic calorimeters for photon detection. Apart from the shorter target and the corresponding RPD lengths, this set-up has the principal features of the one foreseen for the proposed future GPD programme. DVCS test measurements were performed using both μ^+ and μ^- beams of 160 GeV energy, with an intensity of about 1/3 of the maximum in 2008 and close to the maximum intensity in 2009. The 2008 DVCS test data allowed one to clearly identify exclusive photon production and to obtain a first direct determination of the global overall efficiency. The latter, including also SPS beam and spectrometer availabilities, trigger and DAQ efficiencies, was found to be close to the value of 10% assumed for the projections. The 2009 DVCS tests data provided a first direct measurement of the relative con-

tributions of the BH and DVCS in the x_B domain available at COMPASS (Fig. 5). Note that the predicted ϕ dependence of the DVCS cross section is not flat in ϕ due to acceptance effects in the 2009 set-up as there is no electromagnetic calorimeter at large photon angles. This will be improved by the addition of the new calorimeter ECAL0 already mentioned above.

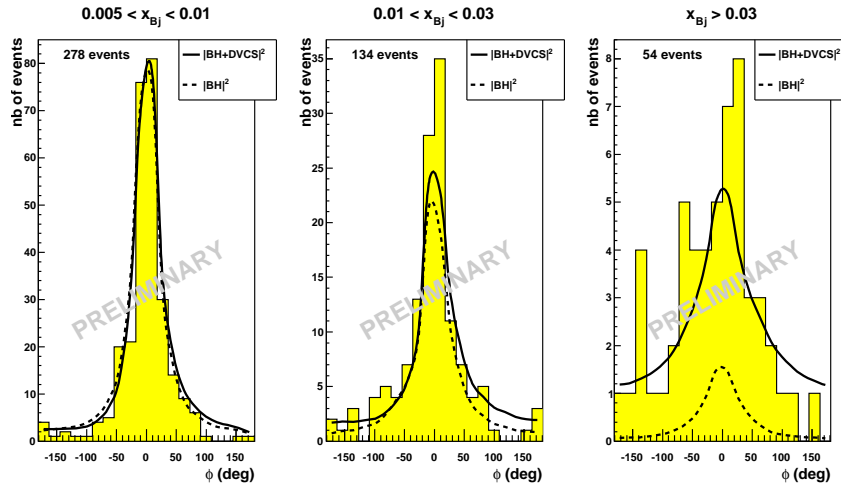


Figure 5. Distribution in the azimuthal angle ϕ for measured exclusive single-photon events, $\mu p \rightarrow \mu' p \gamma$ with $Q^2 > 1 \text{ GeV}^2$, in the same three x_B bins as in Fig. 1. Shown here is a Monte Carlo simulation of only the BH process ($|\text{BH}|^2$) and of both the BH and DVCS processes ($|\text{BH} + \text{DVCS}|^2$).

References

1. COMPASS-II proposal, SPSC-P-340, <http://cdsweb.cern.ch/record/1265628/files/SPSC-P-340.pdf>, May 17, 2010
2. A.V. Belitsky, D. Müller and A. Kirchner, Nucl. Phys. B **629** (2002) 323.
3. M. Vanderhaeghen, P.A.M. Guichon and M. Guidal, Phys. Rev. Lett. **80** (1998) 5064; Phys. Rev. D **60** (1999) 094017; K. Goeke, M.V. Polyakov and M. Vanderhaeghen, Prog. Part. Nucl. Phys. **47** (2001) 401.
4. K. Kumericki, D. Mueller and K. Passek-Kumericki, Nucl. Phys. **B 794** (2008) 244, K. Kumericki and D. Mueller, arXiv 0904.0458[hep-ph]
5. H1, A. Aktas *et al.*, Eur. Phys. J.C **44** (2005) 1, F.D. Aaron *et al.*, Phys. Lett. B **659** (2008) 796.
6. ZEUS, S. Chekanov *et al.*, DESY-08-178, arXiv:hep-exp:0812.2517v3.
7. M. Diehl, Th. Feldmann, R. Jakob and P. Kroll, Eur. Phys. J. C **39** (2005) 1.
8. M. Guidal, M.V. Polyakov, A.V. Radyushkin and M. Vanderhaeghen, Phys. Rev. D **72** (2005) 054013.